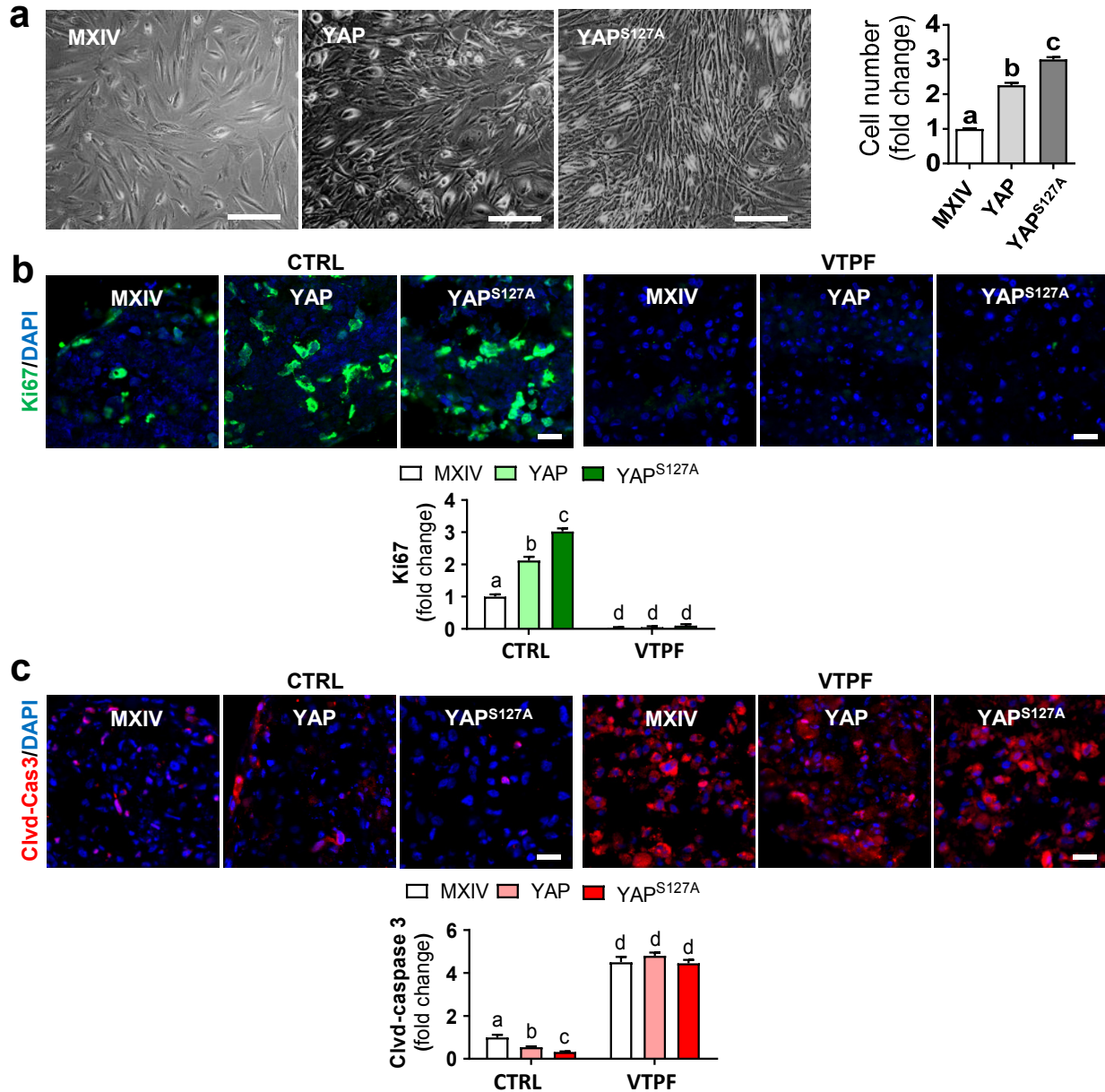
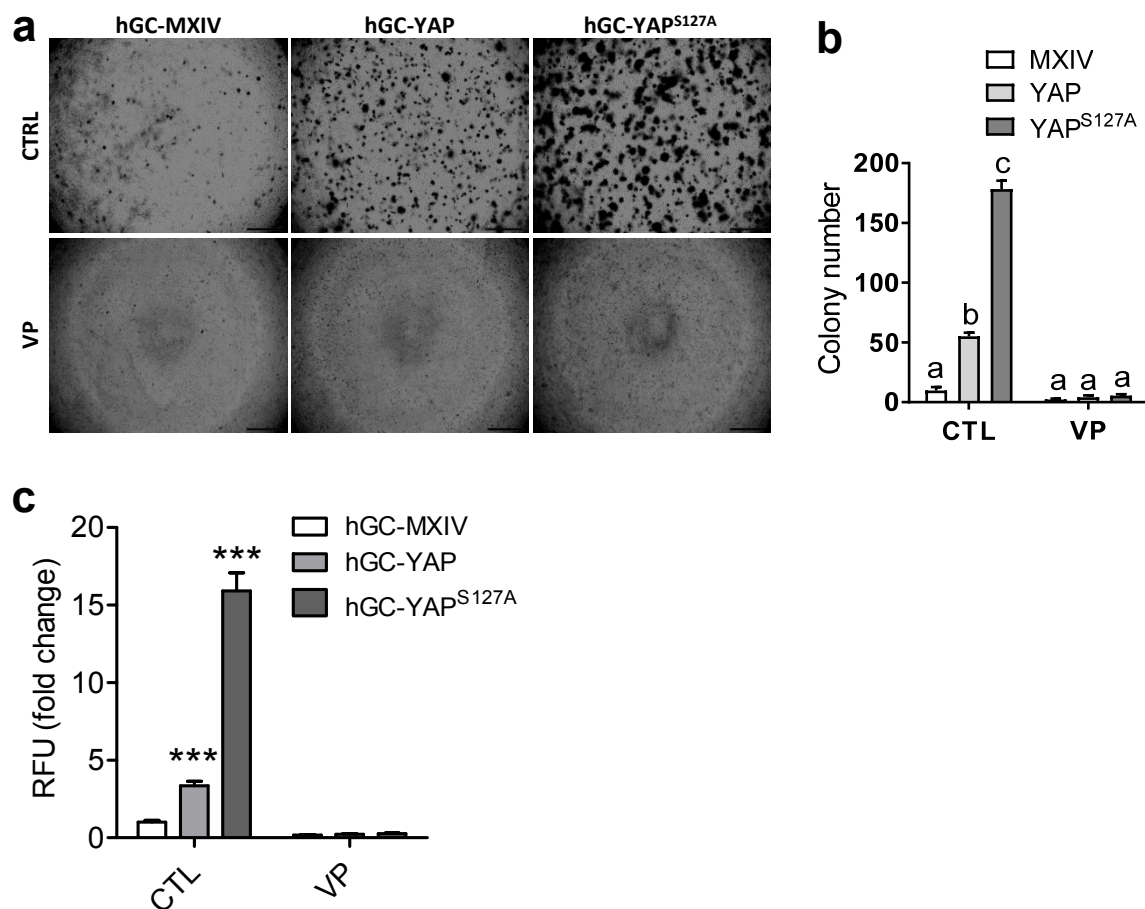


## Supplementary Figure



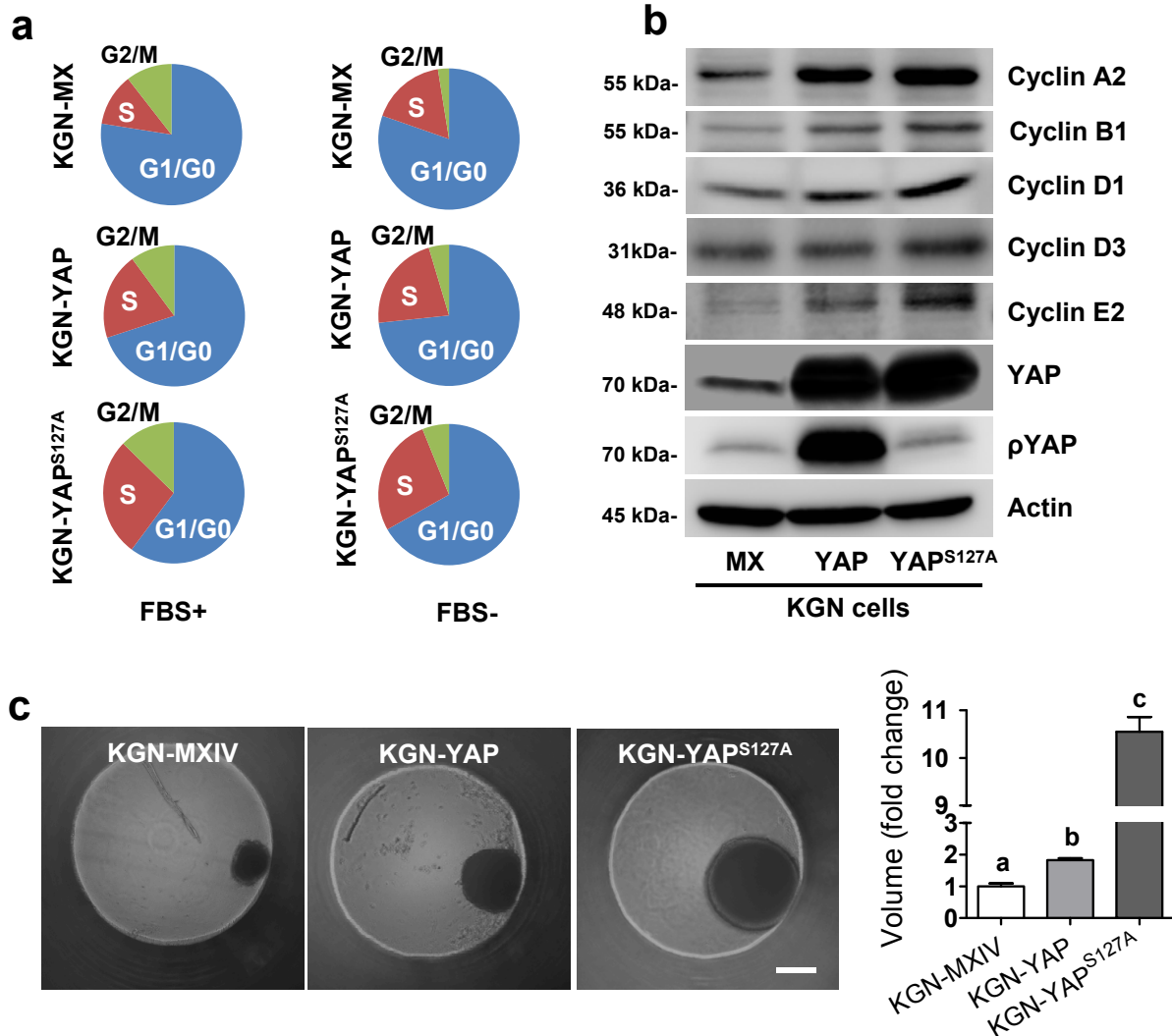
**Supplementary figure S1. YAP1 promotes proliferation and supports survival of human granulosa cells.** **a)** Representative images showing morphology of control MXIV, **YAP**, and **YAP<sup>S127A</sup>**-expressing hGCs incubated in the growing medium for 5 days, Scale bar: 200  $\mu$ m; right: bar graph showing cell number change of control and YAP1-expressing hGCs incubated in the growing medium for 5 days. Each bar represents the mean  $\pm$  SEM ( $n = 4$ ). Bars with different letters are significantly different from each other ( $P < 0.01$ ). **b)** Representative images showing Ki67 expression examined by fluorescent immunohistochemistry in spheroids formed by hGC-MXIV, **hGC-YAP**, and hGC-**YAP<sup>S127A</sup>** cells incubated in the presence or absence of 2  $\mu$ M verteporfin (VP) for 5 days. Scale bar: 20  $\mu$ m. The bar graph shows the quantitative relative ratio of Ki67-positive cells. **c)** Representative images showing cleaved caspase 3 (Clvd-Cas 3) examined by fluorescent immunohistochemistry in spheroids formed by hGC-MXIV, **hGC-YAP**, and hGC-**YAP<sup>S127A</sup>** cells incubated in the presence or absence of 2  $\mu$ M verteporfin for 5 days; The bar graph showing the relative ratio of cells with cleaved caspase 3. Scale bar: 20  $\mu$ m. Each bar represents the mean  $\pm$  SEM ( $n \geq 4$ ). Bars with different letters are significantly different from each other ( $P < 0.05$ ).

## Supplementary Figure



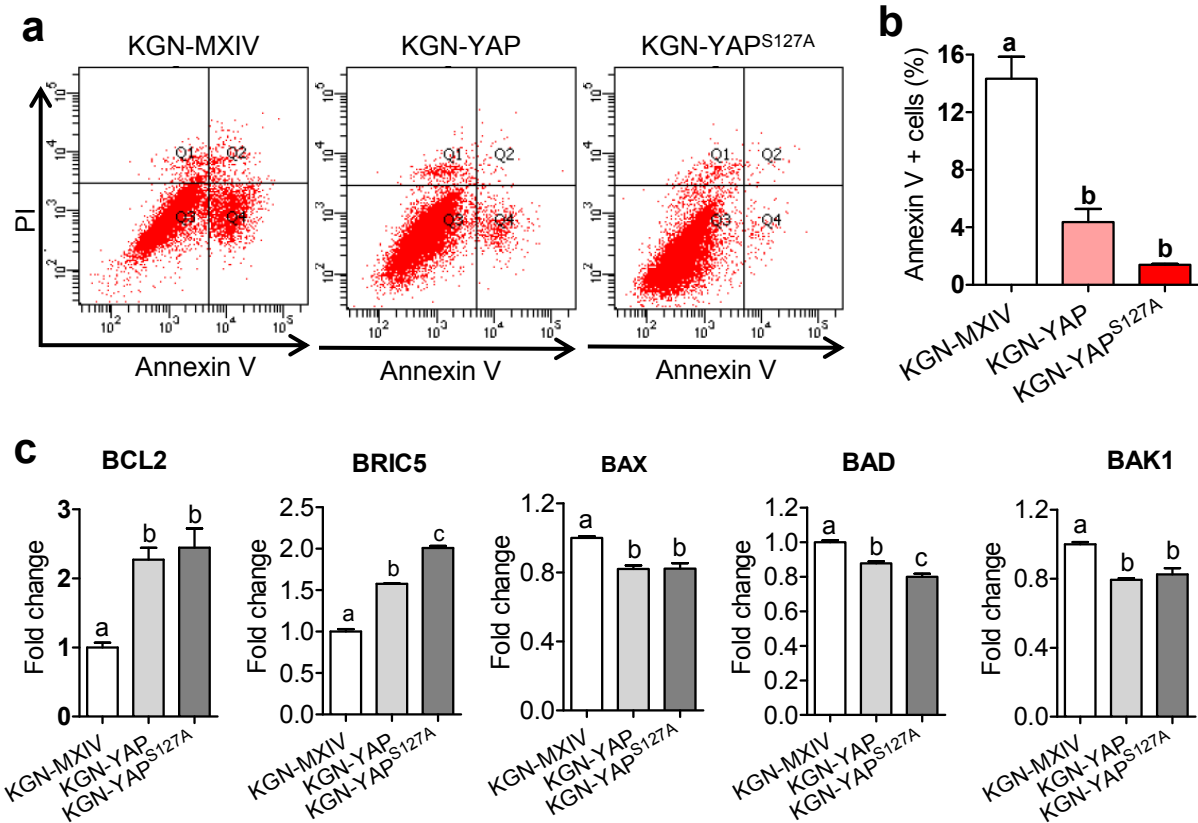
**Supplementary figure S2. Hyperactivation of YAP1 is able to transform primary cultured human granulosa cells (hGCs).** **a)** Representative images showing colonies formed by hGC-MXIV, hGC-YAP, and hGC-YAP<sup>S127A</sup> cells. Cells were incubated in growth medium in a soft agar assay system in the presence or absence of verteporfin (2  $\mu$ M) for 10 days before colony counting. Scale bar: 500  $\mu$ m. **b)** Bar graph showing quantitative data of **a)**. Each bar represents the mean  $\pm$  SEM ( $n = 4$ ). \*\*\*: significantly different from control ( $P < 0.001$ ). **c)** Quantitative analyses of colony formation of hGCs with differential expression of YAP1. hGC-MX, hGC-YAP, or hGC-YAP<sup>S127A</sup> cells were incubated in growth medium in a fluorescence-based semi-quantitative soft agar assay in the presence or absence of verteporfin (2  $\mu$ M) for 10 days. Relative colonies formed by these cells were indicated by relative fluorescence unit (RFU). Each bar represents the mean  $\pm$  SEM ( $n = 4$ ). Bars with different letters are significantly different from each other ( $P < 0.05$ ).

## Supplementary Figure



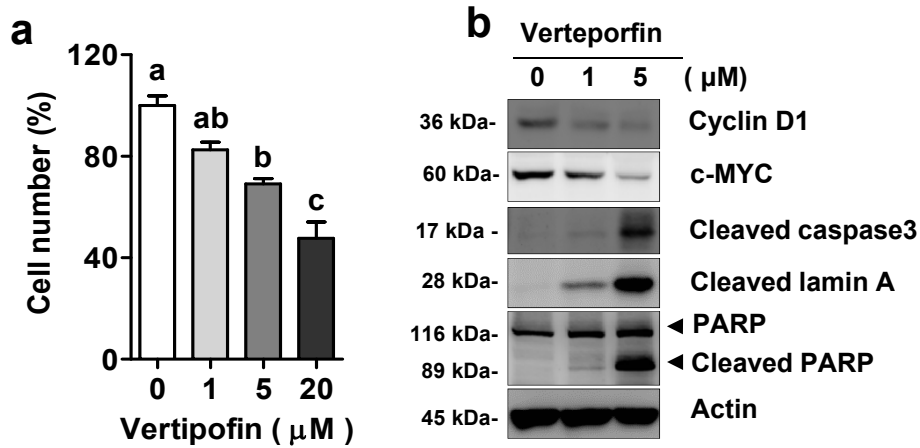
**Supplementary figure S3. YAP promotes the proliferation of KGN cells.** **a)** Ectopic expression of YAP or constitutively active YAP (YAP<sup>S127A</sup>) promotes cell cycle progression in KGN cells. KGN-MXIV, KGN-YAP and KGN-YAP<sup>S127A</sup> cells were cultured in growth medium supplemented with (FBS+) or without (FBS-) serum for 5 days. Cell cycle were analyzed by Annexin V-FITC/PI - based flow cytometry. Experiments were repeated for three times and the representative graphs for each group were presented. **b)** Representative blots showing the protein expression levels of Cyclins in KGN cells after ectopic expression of YAP or constitutively active YAP (YAP<sup>S127A</sup>). Experiments were independently repeated for at least 3 times. **c)** YAP overexpression promotes KGN cell growth in 3D culture: representative pictures showing the spheroids from KGN-MX, KGN-YAP, and KGN-YAP<sup>S127A</sup> cells; bar graph showing quantitative data for the volume of spheroids. Scale bar: 200  $\mu$ m. Graph on the right is the quantitative data of the volume of the KGN cell spheroid in each group. Each bar represents the mean  $\pm$  SEM ( $n \geq 5$ ). Bars with different letters are significantly different from each other ( $P < 0.05$ ).

## Supplementary Figure



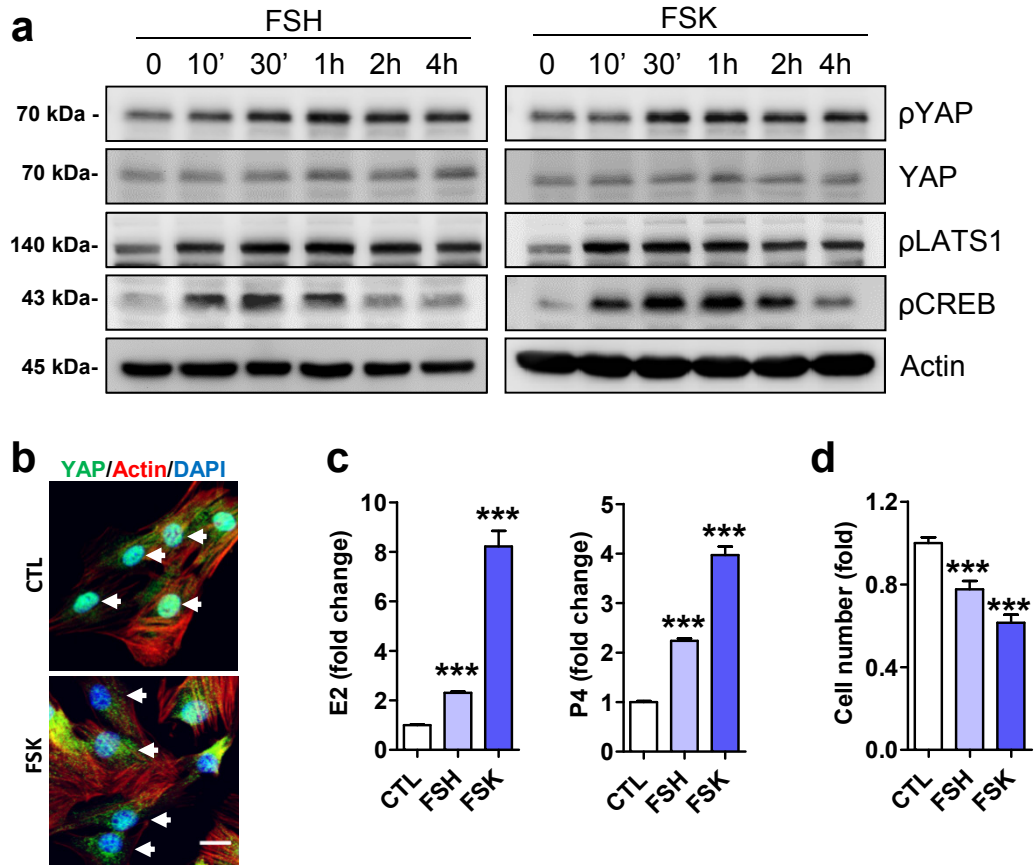
**Supplementary figure S4. YAP plays important role in regulating KGN cell survival.** **a)** Representative pictures showing Annexin V-FITC/Propidium Iodide (PI) double staining of KGN-MX, KGN-YAP, and KGN-YAP<sup>S127A</sup> cells after serum starvation for 4 days. **b)** Quantitative results of **a)**. Each bar represents mean + SEM of 3 independent experiments. Bars with different letter are significantly different from each other ( $P < 0.05$ ). **c)** *BCL2*, *BRIC5*, *BAX*, *BAD*, and *BAK1* mRNA expression levels in KGN-MX, KGN-YAP, KGN-YAP<sup>S127A</sup> cells were detected by RT-PCR. Each bar represents the mean  $\pm$  SEM ( $n \geq 3$ ). Bars with different letters are significantly different from each other ( $P < 0.05$ ).

## Supplementary Figure



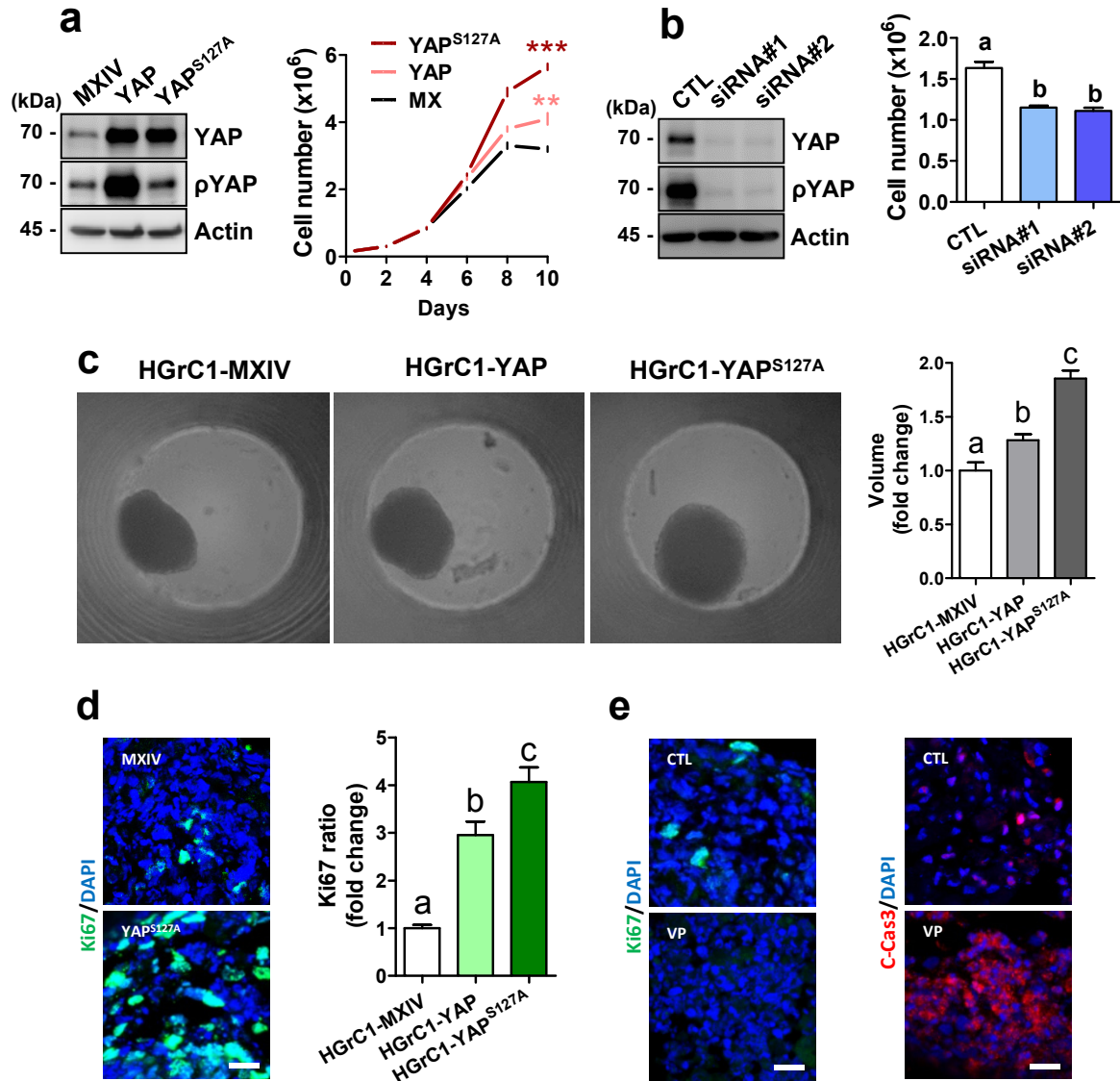
**Supplementary figure S5. YAP plays important role in the proliferation and apoptosis of KGN cells.** a) YAP inactivation by verteporfin inhibits KGN cell growth: the bar graph showing KGN cell number after incubating in growth medium with increasing concentrations of verteporfin for 5 days. Each bar represents the mean  $\pm$  SEM ( $n \geq 3$ ). Bars with different letters are significantly different from each other ( $P < 0.05$ ). b) Western blot results showing expression changes of cell proliferation markers and apoptosis markers with different concentration of verteporfin treatment for 5 d.

## Supplementary Figure



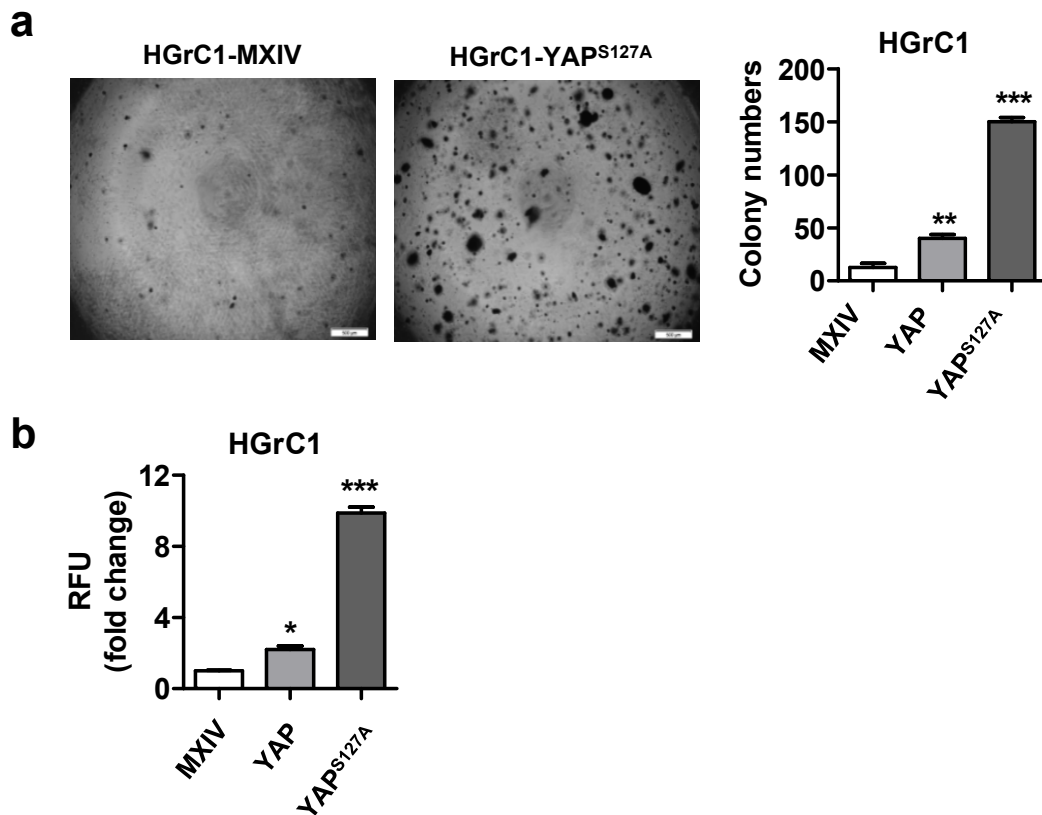
**Supplementary figure S6. FSH and FSK activated the Hippo pathway to suppress YAP activity and induced hormone production, and inhibited cell proliferation.** **a**) FSH (10 ng/ml) and forskolin (FSK, 10  $\mu$ M) treatment induced phosphorylation of YAP and LATS1 in KGN cells. Phosphorylated CREB was used as a positive control of FSH and FSK action.  $\beta$ -actin was used as a protein loading control. **b**) FSK treatment (10  $\mu$ M, 60') suppresses YAP activity by retaining YAP in the cytoplasm. YAP protein was stained by fluorescent immunohistochemistry and visualized by a Alexa 488-conjugated second antibody (green). Actin was stained with phalloidin-rodhamine (red). Nuclei was stained by DAPI (blue). Scale bar = 20  $\mu$ m. **c**) Bar graphs showing production of 17 $\beta$ -estradiol (E2) and progesterone (P4) in KGN cells incubated in growth media for 3 days in the absence (CTL) or presence of FSH (10 ng/ml) or FSK (10  $\mu$ M). **d**) Bar graphs showing growth of KGN cells incubated for 3 days in the growth media in the absence (CTL) or presence of FSH (10 ng/ml) or FSK (10  $\mu$ M). Each bar represents the mean  $\pm$  SEM ( $n \geq 3$ ). \*\*\* :  $P < 0.001$ , compared with control (CTL).

## Supplementary Figure



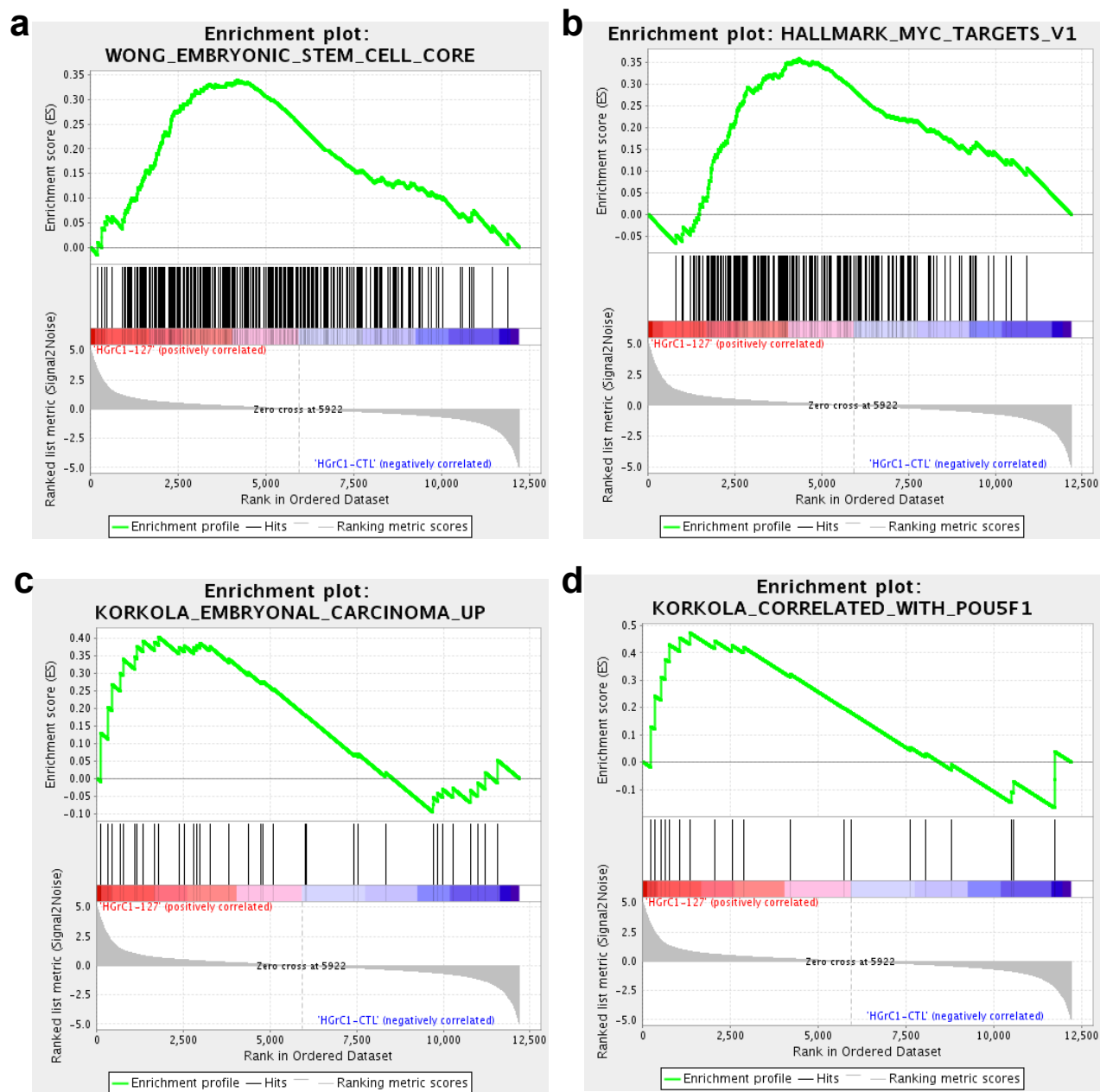
**Supplementary figure S7. YAP1 promotes proliferation and supports survival of HGrC1 cells in both 2D and 3D culture systems. a)** Ectopic expression of YAP1 promotes HGrC1 cell proliferation. Left panel: Western blot showing YAP1 expression in HGrC1-MXIV, HGrC1-YAP, and HGrC1-YAP<sup>S127A</sup> cells; right panel: growth curves of three cell lines. Each point represents the mean  $\pm$  SEM (n = 4). \*\*:  $p < 0.01$ , \*\*\*:  $P < 0.001$ , compared to the control group in the same day (day 10). **b)** knockdown of YAP1 suppresses growth of HGrC1 cells. Left panel: Western blot showing knockdown of YAP1 protein with YAP1-targeting siRNA#1 and siRNA#2; right panel showing cell number changes in HGrC1 cells with or without knockdown of YAP1. HGrC1 cells were transfected with non-targeting RNA (CTL) or YAP siRNA#1 and siRNA#2. Cell number was counted 4d after transfection. Each bar represents the mean  $\pm$  SEM (n = 4). Bars with different letter are significantly different from each other ( $P < 0.05$ ). **c)** Representative pictures showing the spheroids formed by HGrC1-MXIV, HGrC1-YAP, and HGrC1-YAP<sup>S127A</sup> cells in the 3D culture system after loading onto a 3D culture system for 5 days; The bar graph showing relative volume of spheroids. Scale bar: 200  $\mu$ m. **d)** Representative pictures showing Ki67 staining with spheroids formed by HGrC1-MXIV and HGrC1-YAP<sup>S127A</sup> cells; Scale bar: 20  $\mu$ m. bar graph showing ratio of Ki67 positive cells. Each bar represents the mean  $\pm$  SEM (n  $\geq$  4). Bars with different letters are significantly different from each other ( $P < 0.05$ ). **e)** Representative images showing Ki67 (green) and cleaved Caspase 3 (red) expression in spheroids formed by HGrC1 cells cultured in the absence (CTRL) or presence (VP) of verteporfin (2 $\mu$ M) for 5 days. Scale bar: 20  $\mu$ m.

## Supplementary Figure

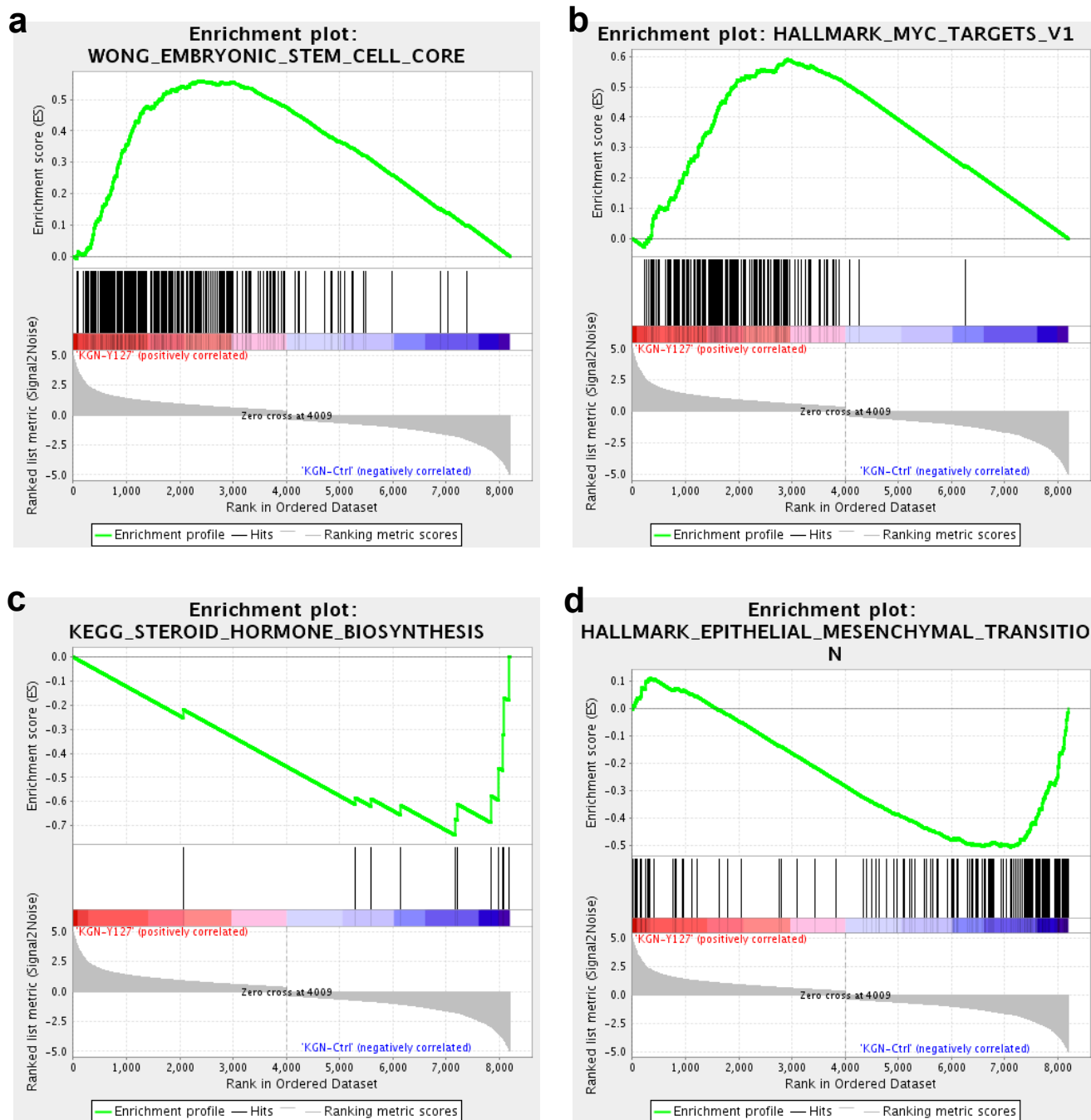


**Supplementary figure S8. YAP1 promotes transformation of HGrC1 granulosa cells.** **a)** Representative images showing colonies formed by HGrC1-MX and HGrC1-YAP<sup>S127A</sup> cells in the soft agar assay. Scale bar: 500  $\mu$ m. Bar graph on the right showing the quantitative data of colonies formed by HGrC1-MX, HGrC1-YAP, and HGrC1-YAP<sup>S127A</sup> cells in the soft agar assay. **b)** Relative colony numbers formed by HGrC1-MX, HGrC1-YAP, and HGrC1-YAP<sup>S127A</sup> cells in a fluorescence-based semi-quantitative colony formation assay. The relative colony number in each cell lines is reflected by relative fluorescent unit (RFU). Each bar represents the mean  $\pm$  SEM ( $n \geq 3$ ), when compared with MXIV control, \*:  $P < 0.05$ , \*\*:  $P < 0.01$ , \*\*\*:  $P < 0.001$ .



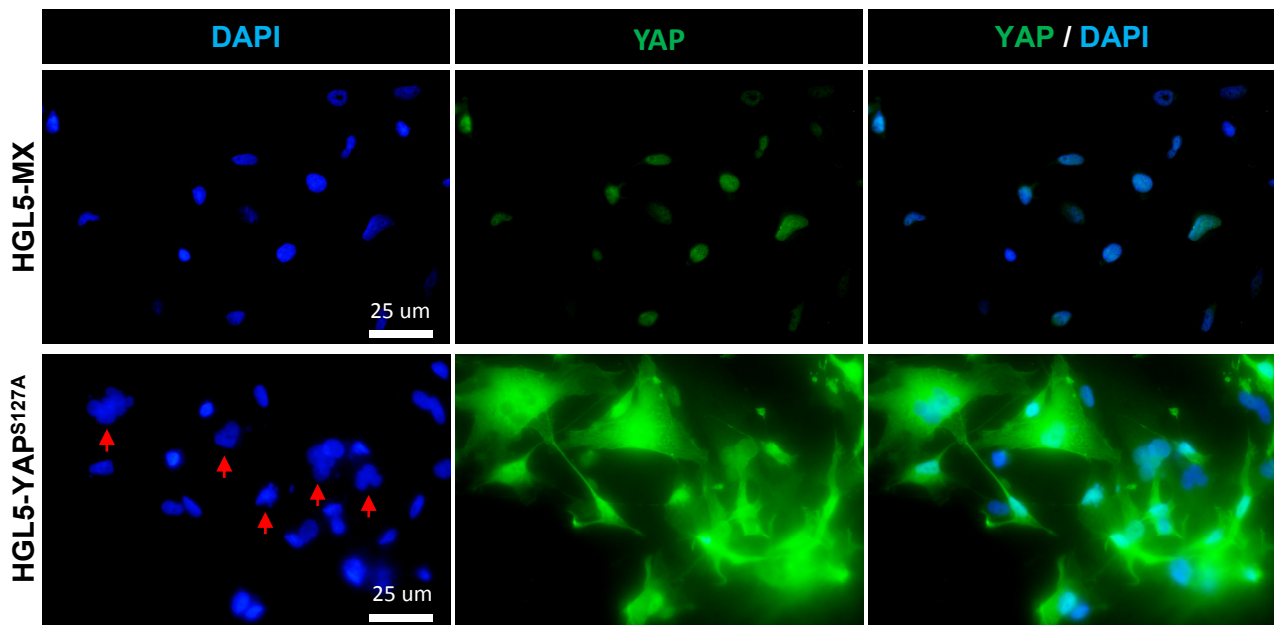


**Supplementary figure S9. YAP1 induced enrichment of genes associated with cellular reprogramming and stemness in HGrC1 cells.** Gene Set Enrichment Analysis (GSEA) was performed based on the gene expression profiling on HGrC1-MX (HGrC1-CTL, n=3) and HGrC1-YAPS127A cells (n=3) using RNA-seq analysis. **a**) Enrichment of genes-associated with embryonic stem cells from the WONG EMBRYONIC STEM CELL CORE gene sets. **b**) Enrichment of genes-associated with cell reprogramming from the HALLMARK MYC TARGETS-V1 gene sets. **c**) Enrichment of genes-associated with development of undifferentiated cancers from the KORKOLA EMBRYONAL CARCINOMA-UP gene sets. **d**) Enrichment of genes-associated with cell reprogramming (Oct4) from the KORLOLA\_CORRELATED\_WITH\_POU5F1 gene sets.



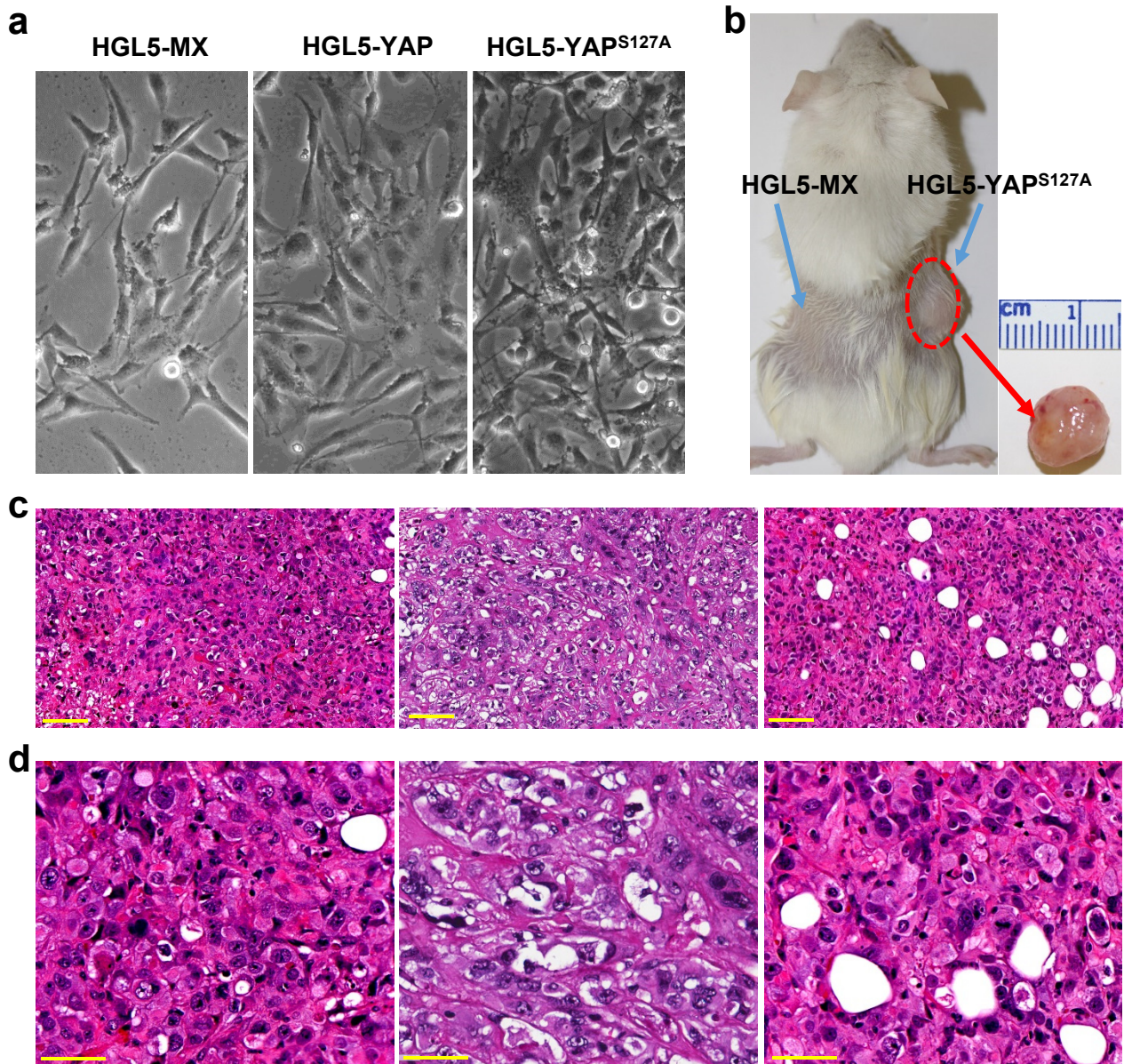
**Supplementary figure S10. YAP1 induced enrichment of genes associated with cellular reprogramming and stemness in KGN cells.** Gene Set Enrichment Analysis (GSEA) was performed based on the gene expression profiling on KGN-MX (HGrC1-CTL, n=3) and KGN-YAPS127A cells (n=3) using RNA-seq analysis. **a)** Enrichment of genes-associated with embryonic stem cells from the WONG EMBRYONIC STEM CELL CORE gene sets. **b)** Enrichment of genes-associated with cell reprogramming from the HALLMARK MYC TARGETS-V1 gene sets. **c)** Enrichment of genes-associated with granulosa cell differentiation from the KEGG\_STEROID-HORMONE\_BIOSYNTHESIS gene sets. **d)** Enrichment of genes-associated with cell reprogramming (MET) from the HALLMARK EPITHELIAL MESENCHYMAL TRANSITION gene sets.

## Supplementary Figure



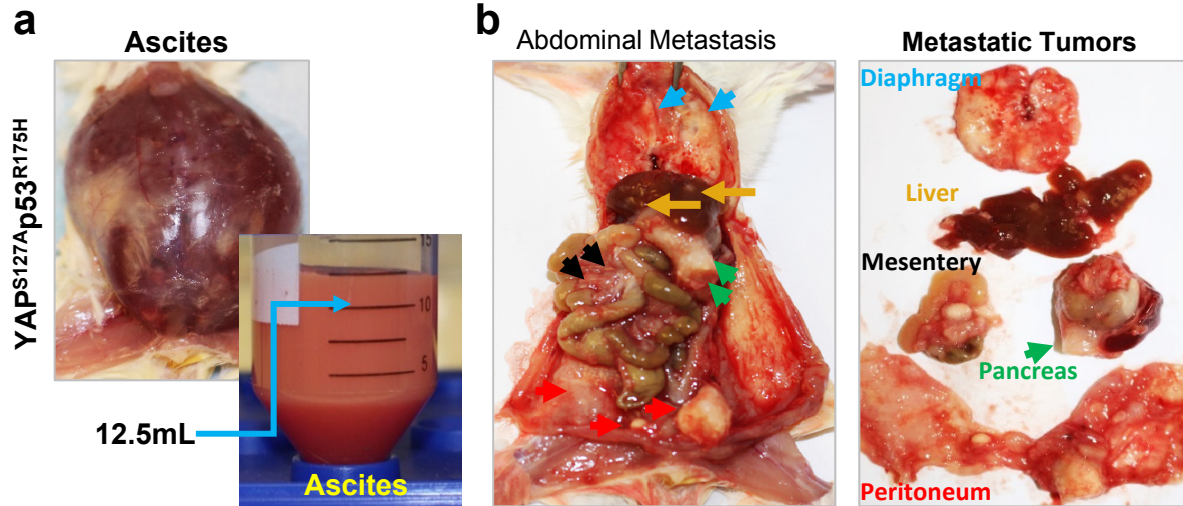
**Supplementary figure S11.** Hyperactivation of YAP1 in HGL5 cells induced significant nuclear atypia. Green signal indicated YAP1 expression detected by fluorescent immunohistochemistry in HGL5-MX (HGL5 cells transfected with empty MXIV vectors as control) and HGL5-YAP<sup>S127A</sup> cells (HGL5 cells transfected with vectors expressing YAP<sup>S127A</sup>, a constitutively active form of YAP1). Nuclei were stained with DAPI (blue). Scale bar: 25μm.

## Supplementary Figure



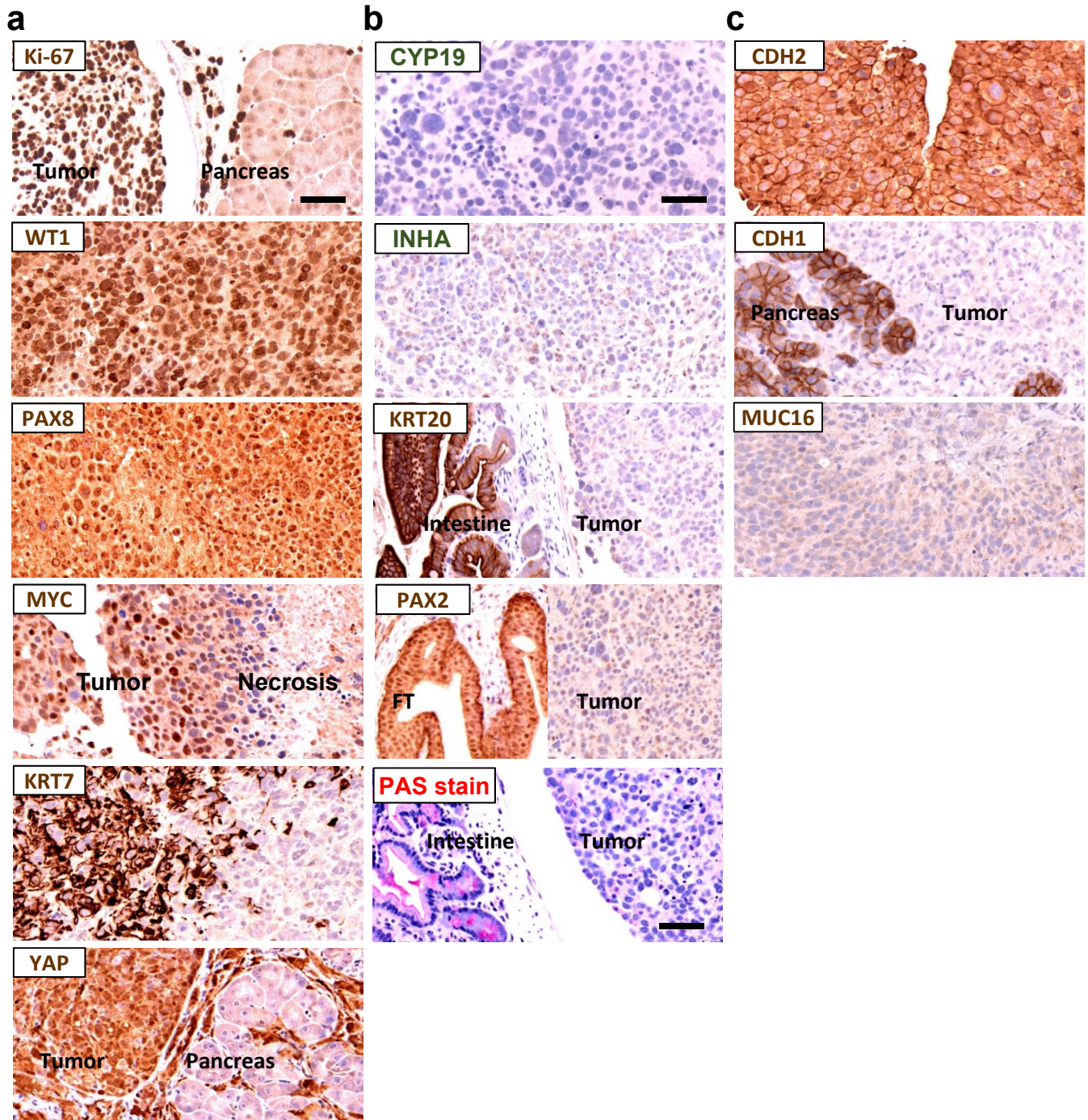
**Supplementary figure S12.** Hyperactivation of YAP1 induced tumorigenesis in the HGL5 cells. **a**) Morphology of cultured HGL5-MX cells (HGL5 cells transfected with empty MXIV vectors as control), HGL5-YAP cells (HGL5 cells transfected with vectors expressing YAP1), and HGL5-YAP<sup>S127A</sup> cells (HGL5 cells transfected with vectors expressing YAP<sup>S127A</sup>, a constitutively active form of YAP1). Please note the rapid multiple layer growth of HGL5-YAP<sup>S127A</sup> cells. Scale bar: 20 $\mu$ m. **b**) HGL5-YAP<sup>S127A</sup> cells, not HGL5-MX cells, formed tumor in NGS mice. **c**) representative low magnification images showing the histology of tumors derived from HGL5-YAP<sup>S127A</sup> cells. Note the nuclear pleomorphism and formation of microcyst. Scale bar: 100 $\mu$ m. **d**) Representative high-resolution images showing the histology of tumors derived from HGL5-YAP<sup>S127A</sup> cells. Note the high pleomorphic nuclei, large with coarsely clumped chromatin, and numerous abnormal mitotic figures. Scale bar: 50 $\mu$ m

## Supplementary Figure



**Supplementary figure S13.** Introduction of  $TP53^{R175H}$  did not affect progression of tumors derived from HGrC1-YAP<sup>S127A</sup> cells. **a)** Representative images showing accumulation of large amount of ascites in the abdomen of mice carrying tumors derived from HGrC1-YAP<sup>S127A</sup>/TP53<sup>R175H</sup> cells. **b)** Representative images showing metastatic spread of tumors derived from HGrC1-YAP<sup>S127A</sup>/TP53<sup>R175H</sup> cells in the mouse abdomen organs and tissues, including peritoneum (red arrowhead), mesentery (black arrowhead), diaphragm (blue arrowhead), pancreas (green arrowhead), and liver (orange arrowhead).

Supplementary Figure



**Supplementary figure S14. YAP elicits ovarian HGSC-like tumor from HGrC1 cells.** a) Molecular features of tumors derived from HGrC1-YAP<sup>S127A</sup> cells. Representative images showing high expression of Ki-67, WT-1, PAX8, MYC, Keratin 7 (KRT7) and YAP1 proteins in tumor tissues detected by immunohistochemistry. Scale bar: 50 μm. b) Representative images showing that tumor tissues are negative for granulosa cell tumor markers (aromatase, inhibin), low-grade serous carcinoma markers (KRT20, PAX2), and PAS staining (Mucinous ovarian carcinoma). c) Representative images showing that tumor tissues express high level of N-cadherin (CDH2), but very low (or undetectable) levels of E-cadherin (CDH1) and CA125 (MUC15), which is the molecular feature of the mesenchymal type of High-grade serous ovarian carcinoma. Scale bar: 50 μm.